Nanomaterials and Polymers Innovations Vol. 1, No. 1 (2025); 40-49
ISSN: 3102-0798 (Online). Available online at www.nepalpolymer.org

Original research article

Synthesis of Zinc Oxide Nanocatalyst and Its Application in Photodegradation of Rhodamine B

Shukra Raj Regmi[1*], Nurul Hoda Khan[1], Narendra Prakash Shawd[1], Dikpal Kumar Shahi[1], Lekha Nath Khatiwada[2], Rameshwar Adhikari[3*]
[1]*Central Department of Biological and Chemical Sciences, Mid-West University, Surkhet, Nepal*
[2]*Department of Customs, Ministry of Finance, Tripureshwar, Kathmandu, Nepal*
[3]*Research Centre for Applied Science and Technology (RECAST), Tribhuvan University, Kirtipur, Kathmandu 44618, Nepal*

Abstract: We synthesized zinc oxide nanoparticles (ZnO-NPs) by the co-precipitation method for the catalytic degradation of Rhodamine B. The obtained nanoparticle was characterized by a UV-visible spectrophotometer, FTIR (Fourier Transform Infra-Red), EDX (Energy Dispersive X-ray), and XRD crystallography. The ZnO-NPs have shown maximum absorbance intensity at 365 nm, and an optical band gap of 3.29 eV based on Tauc plot. The FTIR spectra reveal strong stretching of Zn-O at 779.11 cm^{-1}. The EDX spectra depicted 81.90 % zinc (Zn), and 17.99 % oxygen (O) as an elemental composition. The XRD spectra show hexagonal wurtzite geometry. Solving Scherrer's equation, we obtained the average size of the particle 23.9 nm, and the crystallinity 75.43%. The solar light intensity 5.74±0.14 $kWh/m^2/day$ was used to degrade Rhodamine B completely within 140 minutes with ≈80% catalytic efficiency, and in the dark medium, the degradation is found prolonged up to 220 minutes with ≈15% efficiency. The degradation in heat and light is achieved in 110 minutes at 110 °C. The degradation of dye obeys pseudo-first-order kinetics and the rate constant is obtained at 0.01274 min^{-1} in light. The finding reveals that photocatalytic degradation under controlled temperature is superior to the degradation achieved in light and dark. The mineralization of Rhodamine B demonstrates the potential application of ZnO-NPs as a photocatalyst.

Keywords: photocatalysis, ZnO-NPs, Rhodamine B, dye degradation, nanocatalyst

शोधसार: प्रस्तुत अनुसन्धानमा हामीले रोडामिन बी को उत्प्रेरक क्षयका लागि को-प्रेसिपिटेसन विधिबाट जिंक अक्साइड न्यानोपार्टिकल्स (ZnO-NPs) संश्लेषण गरेका छौं। प्राप्त न्यानोपार्टिकललाई यूभी-भिजिबल स्पेक्ट्रोफोटोमिटर, FTIR (फोरियर ट्रान्सफर इन्फ्रारेड), EDX (एनर्जी डिस्पर्सिभ एक्स-रे), र XRD क्रिस्टालोग्राफीद्वारा विशेषण गरिएको छ। ZnO-NPs ले ३६५ nm मा अधिकतम अवशोषण तीव्रता देखाएको छ र टक प्लटको आधारमा ३.२९ eV को अप्टिकल ब्यान्ड ग्याप पाइएको छ। FTIR स्पेक्ट्राले ७७९.११ cm^{-1} मा Zn-O को बलियो स्ट्रेचिङ देखाउँछ। EDX स्पेक्ट्राले तत्त्वीय संरचना अनुसार ८१.९०% जिंक (Zn) र १७.९९% अक्सिजन (O) रहेको देखाएको छ। XRD स्पेक्ट्राले हेग्जागोनल वुर्टजाइट ज्यामिती देखाउँछ। शेरेरको समीकरण प्रयोग गर्दा, कणको औसत आकार २३.९ nm र क्रिस्टलिनिटी ७५.४३% पाइएको छ। सौर्य प्रकाशको तीव्रता ५.७४±०.१४ $kWh/m^2/day$ प्रयोग गरेर रोडामिन बी लाई १४० मिनेटभित्र पूर्ण रूपमा क्षय गरिएको छ, जसमा ≈८०% उत्प्रेरक दक्षता देखिएको छ; अन्धकार वातावरणमा क्षय प्रक्रिया २२० मिनेटसम्म विस्तार भएको छ र दक्षता ≈१५% मात्र देखिएको छ। ताप र प्रकाशमा भने क्षय ११०°C मा ११० मिनेटभित्र सम्पन्न भएको छ। रङको क्षय प्रक्रियाले स्यूडो-प्रथम-अर्डर काइनेटिक्स पालना गर्छ र प्रकाशमा क्षय दर स्थिरांक ०.०१२७४ प्रतिमिनेट पाइएको छ। अनुसन्धानले देखाउँछ कि नियन्त्रित तापक्रममा गरिएको फोटोउत्प्रेरक क्षय प्रक्रियाले केवल प्रकाश वा अन्धकारमा गरिएको क्षयभन्दा उत्कृष्ट परिणाम दिन्छ। रोडामिन बी को मिनरलाइजेसनले ZnO-NPs लाई फोटोउत्प्रेरकको रूपमा प्रयोग गर्न सकिने सम्भावना देखाएको छ।

INTRODUCTION

Zinc oxide is a naturally intrinsic n-type semiconductor having a wide band gap of 3.37 eV (1). It is considered one of the most promising nanocompounds in the multidisciplinary field, and it is used in industries, medicine, electrical

Corresponding authors, E-mails: shukra.regmi@mu.edu.np (SRR) and nepalpolymer@yahoo.com (RA)

Received: April 18, 2025; Revised: May 5, 2025; Accepted: May 12, 2025; Published: May 19, 2025

appliances, advanced semiconducting materials, research, and innovation (2). Zinc oxide-based nano derivatives have revolutionized the world with their tremendous applications in each field, including the polymer industry, drug design, pollutant remover, sensors, cosmetic products, and anti-cancerous and photosensitive products (3). The burgeoning use of ZnO-NPs has made an inalienable bond between technology and human welfare (4). The cost-efficient and less toxic nature of ZnO-NPs synthesis has made the research community a favorite nanomaterial in different research fields. The high electron mobility and wide band gap have made the ZnO-NPs a unique semiconductor, so; it is kept as one of the most prominent and promising candidates in material science (5).

Recently, different techniques are frequently used for the synthesis of ZnO-NPs, including precipitation/co-precipitation, hydrothermal technique, physical vapor deposition, impeded laser beam, sol-gel method, green synthesis, thermal decomposition, spray pyrolysis, and various mechano-chemical processing (6). The common approach applied in the synthesis of ZnO-NPs is the precipitation method. Reports have shown that different precursor concentrations based on zinc acetate $Zn(CH_3COO)_2.2H_2O$, zinc nitrate ($ZnNO_3$), zinc chloride ($ZnCl_2$), zinc sulphate ($ZnSO_4$) with appropriate stabilizers like gelatin, starch, DEA (diethanolamine), under suitable temperature give fine ZnO-NPs with variable shape and size. The precursor solution of zinc sulphate and sodium hydroxide, when vigorously shaken and followed by calcination, gives fine ZnO-NPs (7). Another report has shown that a mixture of zinc salt with precipitant NaOH in an ethanol solution stirred at 9 0°C for 1 hour gives ZnO nanorods (8). A similar process for the solvothermal process gives 33±2 nm, and 48±7 nm ZnO-NPs by taking $Zn(NO_3)_2.6H_2O$ precursor with ethanol solution (9). Another faster and cost-efficient method shows that 0.1 M concentration of zinc acetate dihydrate with propanol boiling with constant stirring at 70 °C turns into a milky solution, which is stabilized by 5-6 drops of DEA (diethanolamine), giving a transparent solution. The spin coating on the substrate by heating the film at 120°C for 5 minutes and annealing at 350°C for 15 minutes gives ZnO thin film (10).

For the synthesis of ZnO-NPs, different factors should be maintained under the laboratory parameters such as the concentration of precursor, pH of the solution, aging of the solution while stirring and settling precipitation, purification, and finally drying (11). These factors generally control the shape, size, crystallinity, and morphology of the particles. Reports show that the precursor concentration highly influences the formation of particle size. High precursor concentration increases the rate of nucleation of the particle and enhances the chance for the formation of smaller nanoparticles, which increases surface reactivity by affecting the surface area to volume ratio. Sensing and catalytic properties are determined by the smaller particles (12,13). Moreover, low precursor concentration forms larger nanoparticles and reduces the chances of nucleation under controlled circumstances; as a result, less reactive particles with a smaller surface area to volume ratio are obtained (14). Size and morphology maintenance is another tedious task in ZnO-NPঘ synthesis. Higher precursor concentrations increase the chances of aggregation to get fine and homogeneous particles; however, irregular and non-crystalline particles are synthesized by the low precursor concentration due to low agglomeration. Precursor concentration also affects the optoelectronic properties, band gap energy, and size of particles (15). In the present work, we have synthesized ZnO-NPs for the catalytic degradation of Rhodamine B under controlled pH conditions to compare the catalytic efficiency with existing parameters.

Although we have existing studies to explore photocatalytic degradation by ZnO-NPs in different parameters, controlled pH with tailored temperature-based synthesis is specifically remarkable. Such a method provides the variation in size of the particle, is easy to control, and allows the formation of defect-free particles. The pure ZnO-NPs effectively show their optical property, which avoids possible recombination. This study aims to degrade Rhodamine B to establish the catalytic strength in controlled laboratory parameters. The fundamental rationale for choosing Rhodamine B is considering it as a model pollutant dye. The excess

use of Rhodamine B in textile, leather, dye industry, biological processing, as a tracer in underground water flow, biological strain, and florescent has made the water resources a pollutant. In the present work, our objective is to investigate the minimum quantity of ZnO-NPs requirement for the effective mineralization of dye for the purification of wastewater(16–19).

MATERIALS AND METHODS

Materials

Zinc acetate dihydrate ($Zn(CH_3COO)_2.2H_2O$, CAS no. 5970-45-6, 219.50 g/M, 98.5 %) and sodium hydroxide (NaOH, CAS no. 1310-73-2, 40 g/M, 97 %) were purchased from Qualigen, India. Polyethylene glycol (PEG, $HO(C_2H_4O)_n^7H$, 100 g/L, CAS no. 25322-68-3) was purchased from Merc, India. Ethanol (C_2H_5OH, 99.99 %, 46.06 g/M, CAS no. 64-17-5) was purchased from Fusion Biotech, India. Rhodamine B ($C_{28}H_{31}CIN_2O_3$, 479.02 g/M, CAS no. 81-88-9) was purchased from Sigma, Aldrich Chemicals, Pvt., India.

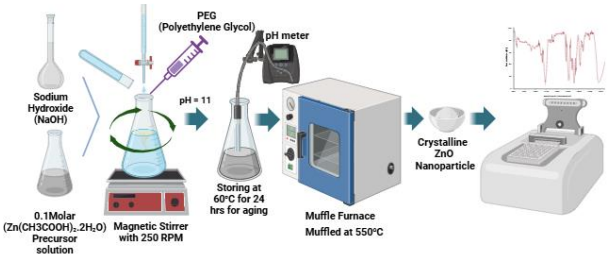

Figure 1. The schematic representation for the synthesis pathway of ZnO-NPs and its characterization.

The overall research design of the present project is depicted in Fig. 1. The decimolar zinc acetate dihydrate precursor was prepared by adding 21.95 g in 1L deionized distilled water. Similarly, decimolar sodium hydroxide was prepared by dissolving 4 gm in 1L water. Both solutions were stirred for 20 minutes at 25°C. The process was achieved by dropping sodium hydroxide from the burette until the pH of the solution was maintained at 11, at constant stirring of 250 rpm in 50 mL zinc acetate solution. The synthetic pathway is carried out by the formation of zinc hydroxide. The polyethylene glycol (PEG) was added continuously dropwise to avoid the agglomeration of the precipitate mass. After 1 hour of stirring in a thermoregulatory stirrer, the mass was kept for one hour at room temperature for aging. The process was followed by keeping the obtained mass at 80°C in a hot-air oven. The dry zinc hydroxide mass was scrapped and kept on a silica crucible for calcination at 550 °C. The dry crystalline white powder obtained is represented as ZnO-NPs in the experiment, which was stored in a dry borosilicate airtight container.

Characterization of ZnO-NPs

The synthesized zinc oxide nanoparticles (ZnO-NPs) are characterized by modern spectroscopic techniques. The UV-visible spectrophotometer (UV-1900i, Shimadzu, Japan) was used to find out the maximum absorbance of the nanoparticle. The Fourier-Transform Infrared Spectroscopy (FTIR, IR Affinity-1s, Shimadzu, Japan) was used to find out the vibrational spectra of the zinc oxide bond. The energy-dispersive X-ray (EDX-8000, Shimadzu, Japan) was used to find out the elemental composition of the nanoparticles. The crystallographic indices of the nanoparticle were obtained by XRD (Bruker, D2 Phaser, Massachusetts, USA).

Photocatalytic activity of ZnO-NPs

Photocatalytic degradation was achieved in the solar light having an intensity of 5.64 ± 0.14 kWh/m^2/day. The solar intensity is measured by CMP3 pyranometer. Zinc oxide is a semiconductor that absorbs light having an intensity equal to the band gap or greater than the band gap. The ZnO-NPs are an intrinsic n-type semiconductor that absorbs photons that excites the electron from the valence band to the conducting band as a result free electron-hole pairs are formed. These pairs form free radicals and superoxide, which causes the mineralization of dye. Generally, photocatalytic degradation obeys zero-order kinetics, which can be determined by the following relations.

$$-K_t = \ln \frac{C_t}{C_o} \quad \ldots\ldots\ldots\ldots (1)$$

where, 'k_t' = Rate constant for Pseudo-First-Order Kinetics, 'C_t' = Concentration of dye at the time't', and 'C_o' = Initial concentration of dye.

The following relation calculates the catalytic efficiency (20).

$$\text{Degradation (\%)} = \frac{C_o - C_t}{C_o} \quad \ldots\ldots\ldots\ldots (2)$$

The photocatalytic degradation mechanism can be explained in the following chemical equations.

$$\text{ZnO-NPs} \xrightarrow{h\nu} \text{ZnO}(e^-)_{CB} + \text{ZnO}(H+)_{VB} \quad \ldots(3)$$

$$\text{ZnO(Hole+)}_{VB} + H_2O \rightarrow H^+ + OH^- \text{ (ions)} \quad \ldots(4)$$

$$\text{ZnO (Hole+)}_{VB} + OH^- \rightarrow OH \text{ (Radicals)} \quad \ldots(5)$$

$$4OH^- \text{(Solution)} \rightarrow 2H_2O + O_2 \quad \ldots(6)$$

$$\text{ZnO(e-)}_{CB} + O_2 \rightarrow O_2^- \text{(Superoxide)} \quad \ldots(7)$$

$$\text{Rhodamine B} + OH^- \text{(Radical)} \rightarrow CO_2 + H_2O \ldots(8)$$

$$\text{Rhodamine B} + O_2^- \rightarrow CO_2 + H_2O \quad \ldots(9)$$

RESULTS AND DISCUSSION

UV-visible Spectra of ZnO-NPs

The results obtained from the UV-vis spectrophotometry are presented in Fig. 2

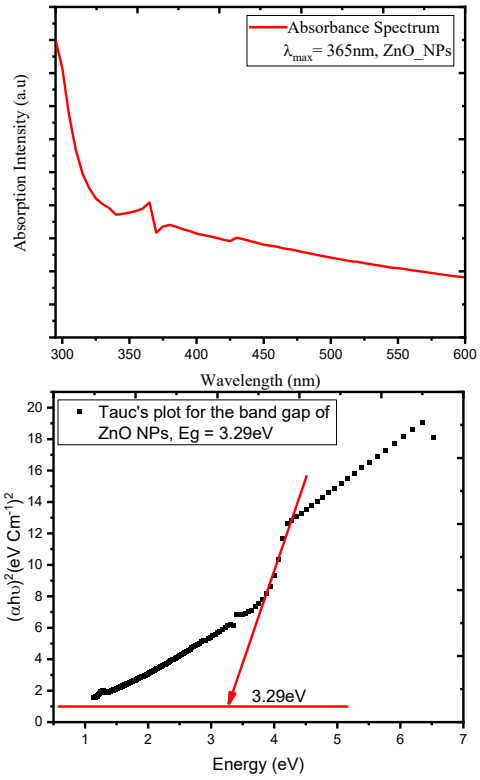

Figure 2: UV-visible spectra of ZnO-NPs showing maximum absorbance at 365 nm (a) and Tauc plot for the determination of band gap of ZnO-NPs showing E_g = 3.29 eV (b).

The maximum wavelength absorbed by ZnO-NPs was found at 365 nm (Fig. 2a). The Tauc plot was obtained based on the absorbance (Fig. 2b). The band gap of ZnO-NPs is found to be 3.29 eV, which is almost equal to the reported band gap (21). The calculation shows that the synthesized ZnO-NPs have a wide band gap but are very efficient in absorbing light. This band gap signifies that the nanomaterial is thermally stable and has a low intrinsic carrier to conduct electricity in the conductance band (22,23). By solving Brus's equation, we obtained the size of particle 1.31 nm at wavelength 365 nm. The optical band gap 3.29 eV is obtained using Tauc plot. The Brus's equation can be defined as:

$$E_{QD} = E_g + \frac{h^2\pi^2}{2R^2}\left(\frac{1}{m_e} + \frac{1}{m_h}\right) - \frac{1.8e^2}{4\pi\epsilon_o\varepsilon R} \quad \ldots\ldots(10)$$

where, 'E_{QD}' is the band energy of quantum dot, 'E_g' is the bulk band gap, 'm_e' and 'm_h' are the mass of electron and hole, ϵ_o is the permittivity of vacuum, and ε is the dielectric constant (24). Tauc's equation is used to calculate optical band gap (25).

$$\alpha h\vartheta = A(h\vartheta - E_g)^n \quad \ldots\ldots\ldots\ldots (11)$$

The energy $h\vartheta$(eV), is calculated as;

$$h\vartheta(\text{eV}) = \frac{1240}{\lambda} \ldots\ldots\ldots\ldots\ldots\ldots\ldots (12)$$

FTIR Spectra Analysis for ZnO-NPs

FTIR analysis of ZnO-NPs shows its characteristic peak in different wavenumbers (Fig. 3). The particles show the trapped water molecule showing its strong O-H stretching in 3448.96 cm^{-1}. Spectra also reveals O-H bending at 1597.83 cm^{-1}.

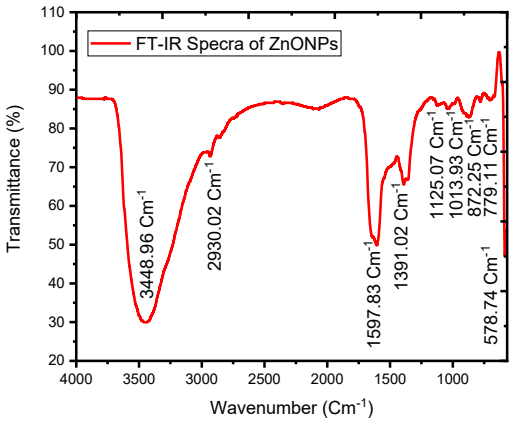

Figure 3: FTIR analysis for zinc oxide nanoparticles (ZnO-NPs)

The small extent of bending found in 2930.02 cm^{-1} shows the stretching of the C-H bond found in the sample, which is due to the precursor of zinc acetate

prepared in organic solvent. The distinct stretching in 578.74 cm^{-1} shows the presence of Zn-O in the sample. The additional bending of Zn-O found in 1013.93, 827.25, 779.11 cm^{-1} confirms the presence of zinc oxide nanoparticles in the sample (26–29).

EDX Analysis for Elemental Composition

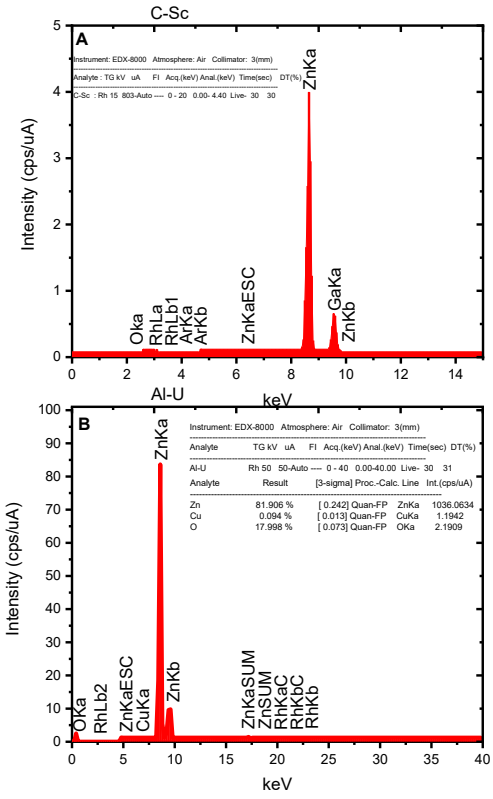

Figure 4: A) EDX spectra of ZnO-NPs showing the elemental composition in C-Sc, and B) EDX spectra of ZnO-NPs showing high resolution of Al-U mode, showing the elemental composition of zinc and oxygen.

The EDX spectra of the samples presented in Fig. 4 reveal that the elemental composition of 81.90% zinc (Zn) and 19.99% oxygen (O). The sharp and significant peak obtained in different energy ranges shows the presence of zinc oxide nanoparticles. The dispersive peak spectra obtained at Al-U mode show the oxygen peak of energy 3.56 keV and Intensity (0.23 cps/uA). Furthermore, the peak of zinc shows an energy of 8.59 keV and an Intensity of 84.63 cps/uA). The peak obtained for zinc with an energy of 9.52 keV, and an intensity of 10.78 also confirms the presence of zinc oxide nanoparticles in the sample (30–32).

XRD Crystallographic Analysis for the ZnO-NPs

Crystallography of ZnO-NPs depicts its sharp peak at the plane 101 (2θ = 35.5°), 111 (2θ = 34.28°), 102 (2θ = 47.30°), 110 (2θ = 56.47°), 103 (2θ = 62.67°), 112 (2θ = 67.79°), 200 (2θ = 68.86°, Intensity 388.37), 201 (2θ = 76.74°, Intensity 106.96), 202 (2θ = 81.23°), 002 (2θ = 29.59°). For ZnO-NPs, the obtained 2θ = 36.5° for 111 plane which gives 0.3185 radians. The FWHM (β) obtained ≈0.35°, and β radians = 0.00611. Solving Scherrer's equation the diameter of the ZnO-NPs gives a crystallite size of 23.9 nm and crystallinity of 75.43 %. The obtained crystalline size and crystallinity confirms the presence of ZnO NPs (33,34)

$$D = \frac{K\lambda}{\beta Cos\theta} = \frac{0.9 \times 1.5406 \times 10^{-10}}{0.00611 \times Cos\ (0.3185)}$$

$$= 2.39 \times 10^{-8}\ \text{meter} = 23.9\ \text{nm}$$

The crystallinity is obtained by the following relation.

$$\text{Crystallinity}(\%) = \frac{\text{Crystalline Area}}{\text{Total Area (Crystalline + Amorphous)}} x100$$

$$= \frac{12759.66}{16914.58} \times 100 = 75.43\%$$

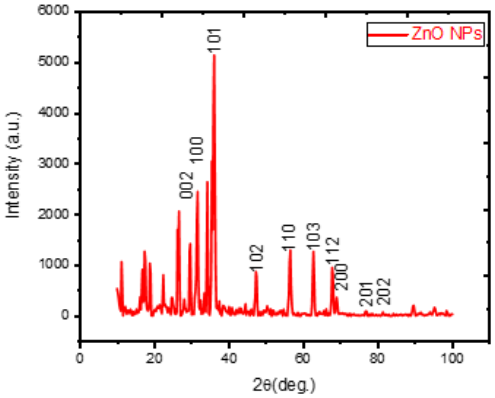

Figure 5: X-ray diffraction pattern of ZnO-NPs.

The X-ray diffractogram of the NPs is presented in Fig. 5. The analysis of the X-RD crystallographic peaks confirms the presence of zinc oxide nanoparticles with wurtzite geometry. The 3D geometric pattern of the particle shows the distinct lattice parameters having bond length (a = 3.22, b = 3.22, c = 5.20), and bond angle (α = 90°, β = 90°, γ = 120°). The unit cell volume for the wurtzite structure is found to be 46.962348 $Å^3$. The three-

dimensional crystal structure of the ZnO-NPs is presented in Fig. 6.

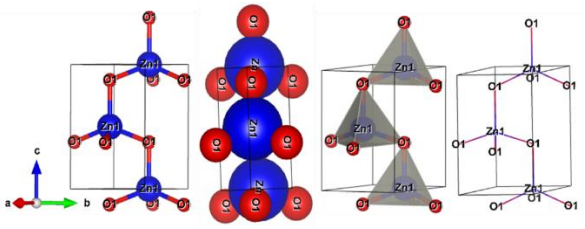

Figure 6: 3D geometric structure of zinc oxide nanoparticles showing the representation in Ball and stick, space-filling, polyhedral, and wireframe structure drawn from VESTA (Visualizing Crystal structures) based on crystallographic open databases (35).

Influence of Light Intensity on ZnO-NPs

Photocatalytic degradation was carried out in the average intensity of light 5.76±0.14 kWh/m^2/day obtained by pyranometer in the days of August 2024. The results are plotted in Fig. 7.

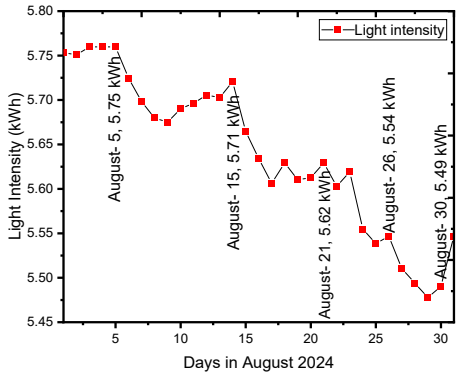

Figure 7: Photo intensity of light in August 2024, obtained by using CMP3 pyranometer in Gurashe, Surkhet, Nepal

The photocatalytic degradation of Rhodamine B was achieved by the action of ZnO-NPs in the presence of light. When ZnO-NPs are added to Rhodamine B dye, the degradation process starts on exposure to light with an intensity of 5.76±0.14 kWh/m^2/day. The degradation process was carried out by adding 10 mg of the NPs in 100 mL of Rhodamine B solution. The degradation mechanism is achieved by the absorption of light by ZnO-NPs that excites the electron from the valence band to the conduction band (see Fig. 8). The process of absorption and excitation of electrons ultimately creates the electron-hole pairs, which convert OH^- ions into $OH^\cdot$ free radical and superoxide O_2^{-}. The free radicals and superoxides are very reactive intermediates that degrade Rhodamine B into simple molecules like CO_2 and H_2O. Hence, mineralization takes place. The degradation process ultimately discharges the pink color Rhodamine B into the colorless solution, that is measured by the intensity of absorbance on the spectrophotometer. The maximum absorption intensity and degradation intensity of Rhodamine B is recorded at a wavelength of 555 nm.

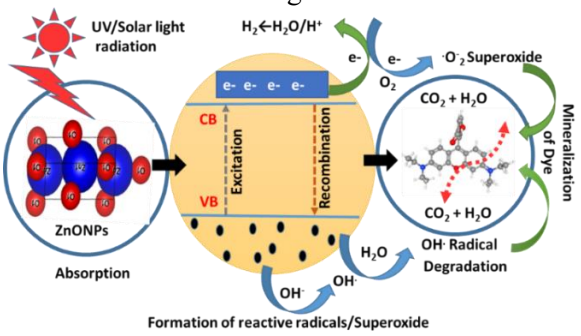

Figure 8: Photocatalytic degradation mechanism of Rhodamine B.

The illustrative mechanism presented in Fig. 8 shows the absorption of photo light, excitation of an electron from the particle surface and formation of holes, formation of hydroxide and superoxide radicals, and recombination and mineralization of dye.

Photocatalytic Degradation of Rhodamine B by ZnO-NPs

The photocatalytic process was carried out by the absorption of photo-light intensity from the exposure of solution over the light having an intensity of 5.76±0.14 kWh/m^2/day. The results are presented in Fig. 9A. Photocatalytic reactions on semiconductor materials like ZnO are very sensitive. Though the calculated band gap is considerably high for the synthesized material, the intensity of solar radiation is huge to generate free radicals and superoxide in the solution. The process is distinctly explained by absorption, excitation, radical and superoxide radical formation, recombination, and mineralization. When 10 mg ZnO-NPs are added to 100 mL of 20 mg/L

Rhodamine B solution in a borosilicate conical flask in exposure to light, the degradation process starts. The initial time at dark was assumed to be zero, and the successive reading was taken in 10 minutes. The light source was not interrupted while the degradation process continued.

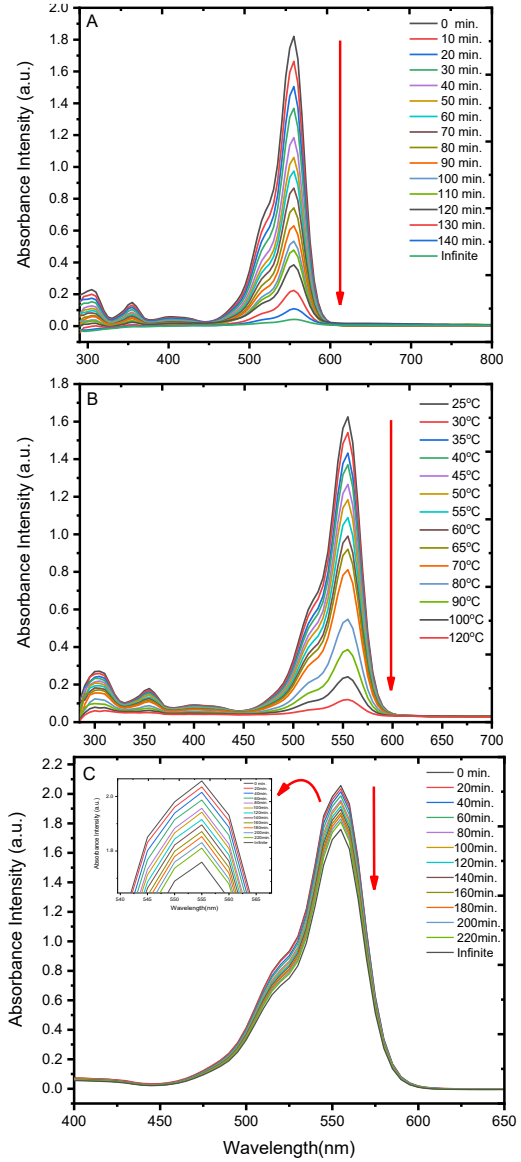

Figure 9: A) Photocatalytic degradation of Rhodamine B in light by ZnO-NPs; B) Photocatalytic degradation of Rhodamine B on increasing temperature by ZnO-NPs, and C) Catalytic degradation of Rhodamine B by ZnO-NPs in dark medium.

The photocatalytic degradation persisted up to 120 minutes for Rhodamine B, which was confirmed by the complete discharge of color and having no absorbance in the spectrophotometer. After the decolorization of pink-colored Rhodamine B, the entire solution was centrifuged at 5400 rpm, where the intact ZnO-NPs settled down at the bottom of the falcon tube that was further used in successive cycles of degradation. Furthermore, the dark medium degradation was achieved by repeating the same process in the absence of light in the dark room (see Fig. 9C). The dark medium degradation was very slow and incomplete up to 220 minutes in consistence with the literature (38,39).

The heating degradation was also achieved in the presence of light. When 10 mg ZnO-NPs were added on 100 mL of 20 mg/L Rhodamine B solution at 25°C, the degradation process was started. The process was continued till the complete degradation occurred for 10-minute intervals in 10 °C difference temperatures (Fig. 9B). The heating degradation was considerably faster than the light and dark medium discharge of Rhodamine B (36,37).

Kinetics of Photocatalytic Degradation for Rhodamine B by ZnO-NPs

The catalytic degradation of Rhodamine B by the ZnO-NPs strictly obeys pseudo-first-order kinetics, as it can be evident from Fig. 10. In the light, the degradation was achieved very fast; the statistical analysis reveals that the linear fitting of $\ln(C/C_o)$ vs. time gives a straight line with a slope -0.01274 and intercept 0.6723 ± 0.0279. The Pearson's 'r' obtained for the degradation is -0.994, with the correlation coefficient (R^2) is 0.989. Similarly, in the dark medium, the degradation was found to fit linearly with a slope of -0.0637 and an intercept of 0.07315 ± 0.02793. The Pearson's coefficient 'r' obtained for dark medium is -0.994 with an adjusted correlation coefficient (R^2) is 0.989, which is equal to the degradation in light. Furthermore, the photocatalytic degradation with the increase in temperature shows the linear fitting with a slope -0.026 ± 0.00058 and intercept of 0.76283 ± 0.11058. The Pearson coefficient 'r' was found -0.9777 with an adjusted correlation coefficient (R^2) is 0.9555.

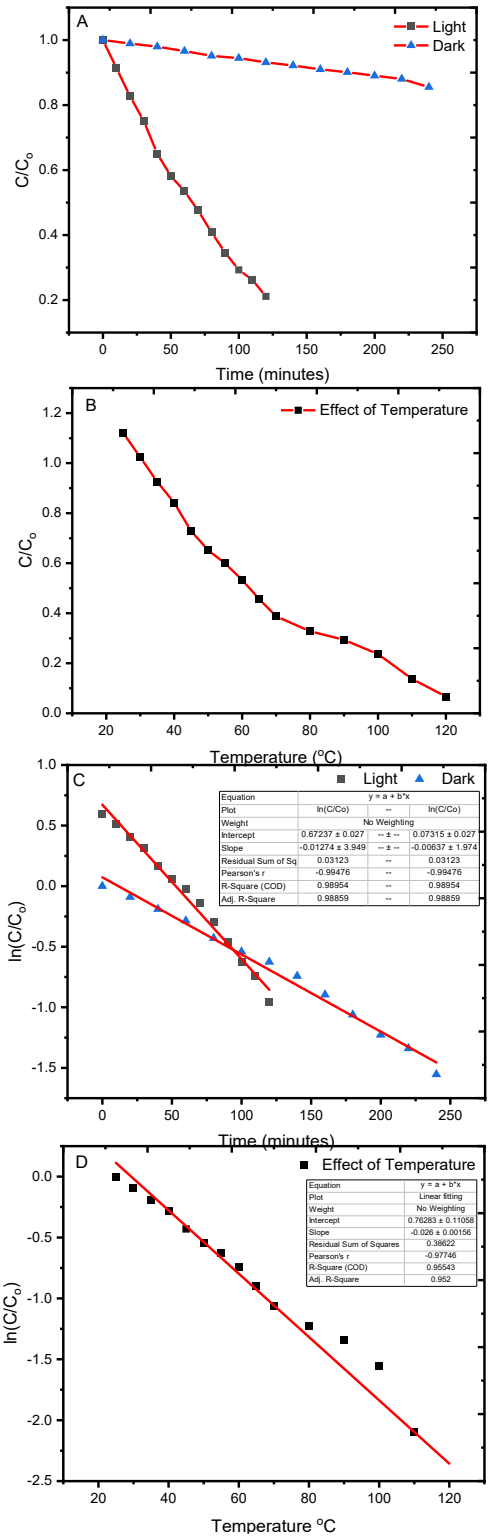

Figure 10: The C/C_o vs time (A), C/C_o vs Temperature (B), and $\ln(C/C_o)$ vs time and temperature plots (C, and D) for the systems studied.

Catalytic Efficiency of ZnO-NPs

The catalytic efficiency of the NPs was calculated by plotting the percentage efficiency versus time (Fig. 11A). For photocatalytic degradation, the efficiency was obtained ≈80% in 120 minutes. Similarly, in the dark, the catalytic efficiency was obtained ≈15% up to 250 minutes, but the efficiency increased ≈90% for the degradation of Rhodamine B in light by heating continuously up to 120 °C (see Fig. 11B).

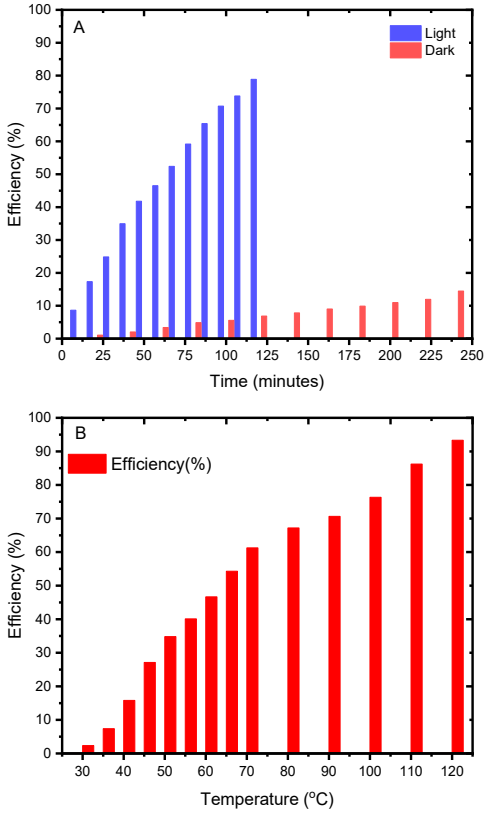

Figure 11: (A) Catalytic efficiency of ZnO-NPs in light and dark, (B). Increased efficiency with temperature in light

Conclusion

The toxicity of dyes on the human body is severe; their degradation into toxic compounds shows several magnitudes of pernicious effects. For the degradation purpose, we synthesized zinc oxide nanoparticles (ZnO-NPs) by the co-precipitation method under controlled pH. The synthesized materials are characterized by a UV-visible spectrophotometer, which gave the maximum absorbance at 365 nm. The band gap was calculated from Tauc's plot, which gave 3.29 eV by the

extrapolation of the obtained plot. The FTIR spectra revealed that Zn-O stretching at 779.11 cm^{-1}. The EDX spectra depicted the elemental composition in the nanoparticles and showed 81.90% zinc (Zn), 17.99% oxygen (O), and trace 0.004 % copper (Cu). The XRD spectra revealed that the ZnO-NPs have wurtzite geometry. On solving Scherer's equation, we obtained the size of particle 23.9 nm and the crystallinity obtained was 75.43 %. The photocatalytic degradation was carried out in 5.74 ± 0.14 kWh/m^2/day light intensity. It was found that the photocatalytic degradation of Rhodamine B obtained in 140 minutes with approximately 80 % catalytic efficiency and in the dark medium, the degradation was very slow and incomplete up to 220 minutes with efficiency ≈15%. The photocatalytic degradation process was completed in 110 minutes at 110ºC. The degradation in dark and light both obey pseudo-first-order kinetics and the rate constant was found to be 0.01274 min^{-1} in light and 0.00637 min^{-1} in dark.

Availability of Data and Materials

The data will be made available at any time when requested.

Funding

No funding was available for this research project.

Author Contributions

SR and NHK: raw materials arrangement, preparation, conducting experiments, and manuscript drafting; NPS: analyzing data, literature survey, DKS: results analysis and interpretation; LNK: EDX analysis and supervision; RA: manuscript editing and supervision.

Conflicts of Interests

The authors declare they have no conflict of interest.

Acknowledgments

The authors would like to acknowledge the Nanotechnology Research Laboratory at RECAST, Tribhuvan University, and Mid-West University, Graduate School of Science & Technology, Chemistry Laboratory, for providing the research facilities. Mr. Ramesh Puri's contribution is highly acknowledged for arranging the UV-spectrophotometer through donation.

REFERENCES

1.Vinitha V, Preeyanghaa M, Vinesh V, Dhanalakshmi R, Neppolian B, Sivamurugan V. Two is better than one: Catalytic, sensing and optical applications of doped zinc oxide nanostructures. Emergent Mater. 2021;4:1093,124.

2.Soriano ML, Zougagh M, Valcárcel M, Ríos Á. Analytical Nanoscience and Nanotechnology: Where we are and where we are heading. Talanta. 2018;177:104–21.

3. Jiang J, Pi J, Cai J. The advancing of zinc oxide nanoparticles for biomedical applications. Bioinorg Chem Appl. 2018;2018(1):1062562.

4. Sun Q, Li J, Le T. Zinc oxide nanoparticle as a novel class of antifungal agents: current advances and future perspectives. J Agric Food Chem. 2018;66:11209–20.

5.Kumar SG, Rao KSRK. Zinc oxide based photocatalysis: tailoring surface-bulk structure and related interfacial charge carrier dynamics for better environmental applications. Rsc Adv. 2015;5:3306–51.

6. Zeb A, Gul M, Nguyen TTL, Maeng HJ. Recent progress and drug delivery applications of surface-functionalized inorganic nanoparticles in cancer therapy. J Pharm Investig. 2023;53(6):743–79.

7. Kumar SS, Venkateswarlu P, Rao VR, Rao GN. Synthesis, characterization and optical properties of zinc oxide nanoparticles. Int Nano Lett. 2013;3:1–6.

8.Oliveira APA, Hochepied JF, Grillon F, Berger MH. Controlled precipitation of zinc oxide particles at room temperature. Chem Mater. 2003;15(16):3202–7.

9. Zak AK, Razali R, Majid WHA, Darroudi M. Synthesis and characterization of a narrow size distribution of zinc oxide nanoparticles. Int J Nanomedicine. 2011;1399–403.

10. Ghimire RR, Mondal S, Raychaudhuri AK. Synergistic ultraviolet photoresponse of a nanostructured ZnO film with gate bias and ultraviolet illumination. J Appl Phys. 2015;117(10).

11.Shaba EY, Jacob JO, Tijani JO, Suleiman MAT. A critical review of synthesis parameters affecting the properties of zinc oxide nanoparticle and its application in wastewater treatment. Appl Water Sci. 2021;11(2):48.

12.Zhang R, Khalizov A, Wang L, Hu M, Xu W. Nucleation and growth of nanoparticles in the atmosphere. Chem Rev. 2012;112(3):1957–2011.

13.An K, Somorjai GA. Size and shape control of metal nanoparticles for reaction selectivity in catalysis. ChemCatChem. 2012;4(10):1512–24.

14. Meulenkamp EA. Synthesis and growth of ZnO nanoparticles. J Phys Chem B. 1998;102(29):5566–72.

15. Ischenko V, Polarz S, Grote D, Stavarache V, Fink K, Driess M. Zinc oxide nanoparticles with defects. Adv Funct Mater. 2005;15(12):1945–54.

16. Chong MN, Jin B, Chow CWK, Saint C. Recent developments in photocatalytic water treatment technology: A review. Water Res [Internet]. 2010;44(10):2997–3027.

tps://www.sciencedirect.com/science/article/pii/S00431
35410001739
17.Dihom HR, Al-Shaibani MM, Radin Mohamed RMS, Al-Gheethi AA, Sharma A, Khamidun MH Bin. Photocatalytic degradation of disperse azo dyes in textile wastewater using green zinc oxide nanoparticles synthesized in plant extract: A critical review. J Water Process Eng [Internet]. 2022;47:102705. Available from: https://www.sciencedirect.com/science/article/pii/S2214714422001489
18.Dodoo-Arhin D, Asiedu T, Agyei-Tuffour B, Nyankson E, Obada D, Mwabora JM. Photocatalytic degradation of Rhodamine dyes using zinc oxide nanoparticles. Mater Today Proc [Internet]. 2021;38:809–15. Available from: https://www.sciencedirect.com/science/article/pii/S2214785320332193
19.Lam SM, Sin JC, Abdullah AZ, Mohamed AR. Degradation of wastewaters containing organic dyes photocatalysed by zinc oxide: a review. Desalin Water Treat [Internet]. 2012;41(1–3):131–69. Available from: https://doi.org/10.1080/19443994.2012.664698
20.Regmi S, Ghimire KN, Pokhrel MR, Khadka DB. Adsorptive removal and recovery of aluminium (III), iron (II), and chromium (VI) onto a low cost functionalized phragmities karka waste. J Inst Sci Technol. 2015;20(2):145–52.
21.Srikant V, Clarke DR. On the optical band gap of zinc oxide. J Appl Phys. 1998;83(10):5447–51.
22.Özgür Ü, Alivov YI, Liu C, Teke A, Reshchikov MA, Doğan S, et al. A comprehensive review of ZnO materials and devices. J Appl Phys. 2005;98(4).
23.Janotti A, Van de Walle CG. Fundamentals of zinc oxide as a semiconductor. Reports Prog Phys. 2009;72(12):126501.
24.Brus L ~E. Electron-electron and electron-hole interactions in small semiconductor crystallites: The size dependence of the lowest excited electronic state. \jcp. 1984 May;80(9):4403–9.
25.Tauc J, Grigorovici R, Vancu A. Optical properties and electronic structure of amorphous germanium. Phys status solidi. 1966;15(2):627–37.
26.Alwan RM, Kadhim QA, Sahan KM, Ali RA, Mahdi RJ, Kassim NA, et al. Synthesis of zinc oxide nanoparticles via sol–gel route and their characterization. Nanosci Nanotechnol. 2015;5(1):1–6.
27.Fakhari S, Jamzad M, Kabiri Fard H. Green synthesis of zinc oxide nanoparticles: a comparison. Green Chem Lett Rev. 2019;12(1):19–24.
28. Kulkarni SS, Shirsat MD. Optical and structural properties of zinc oxide nanoparticles. Int J Adv Res Phys Sci. 2015;2(1):14–8.
29.Tang E, Cheng G, Ma X, Pang X, Zhao Q. Surface modification of zinc oxide nanoparticle by PMAA and its dispersion in aqueous system. Appl Surf Sci. 2006;252(14):5227–32.
30.Das D, Nath BC, Phukon P, Dolui SK. Synthesis of ZnO nanoparticles and evaluation of antioxidant and cytotoxic activity. Colloids Surfaces B Biointerfaces. 2013;111:556–60.
31.Janaki AC, Sailatha E, Gunasekaran S. Synthesis, characteristics and antimicrobial activity of ZnO nanoparticles. Spectrochim Acta Part A Mol Biomol Spectrosc. 2015;144:17–22.
32. Li LH, Deng JC, Deng HR, Liu ZL, Xin L. Synthesis and characterization of chitosan/ZnO nanoparticle composite membranes. Carbohydr Res. 2010;345(8):994–8.
33. Tian ZR, Voigt JA, Liu J, Mckenzie B, Mcdermott MJ, Rodriguez MA, et al. Complex and oriented ZnO nanostructures. Nat Mater [Internet]. 2003;2(12):821–6. Available from: https://doi.org/10.1038/nmat1014
34.Bindu P, Thomas S. Estimation of lattice strain in ZnO nanoparticles: X-ray peak profile analysis. J Theor Appl Phys [Internet]. 2014;8(4):123–34. Available from: https://doi.org/10.1007/s40094-014-0141-9
35. Momma K, Izumi F. VESTA: a three-dimensional visualization system for electronic and structural analysis. J Appl Crystallogr. 2008;41(3):653–8.
36.Varadavenkatesan T, Lyubchik E, Pai S, Pugazhendhi A, Vinayagam R, Selvaraj R. Photocatalytic degradation of Rhodamine B by zinc oxide nanoparticles synthesized using the leaf extract of Cyanometra ramiflora. J Photochem Photobiol B Biol. 2019;199:111621.
37.Sapkota KP, Lee I, Shrestha S, Islam A, Hanif A, Akter J, et al. Coherent CuO-ZnO nanobullets maneuvered for photocatalytic hydrogen generation and degradation of a persistent water pollutant under visible-light illumination. J Environ Chem Eng [Internet]. 2021;9(6):106497. Available from: https://www.sciencedirect.com/science/article/pii/S2213343721014743
38. Shahi DK, Regmi SR, Shawad NP, Khan NH, Joshi PR, Khatiwada LN, Adhikari R. Solar Light Driven Degradation of Methylene Blue by Titanium Oxide Nanoparticles (TiO_2 NPs). J Phys Life Sci. 2023;1(1):21–37.
39. Regmi SR, Khan NH, Shawad NP, Shahi DK, Joshi PR, Chetry AB, Khatiwada LN, Adhikari R. Synthesis of Tin Oxide Nanoparticles (SnO_2 NPs) and its Application in the Photocatalytic Degradation of Waste Alizarin dye. J Phys Life Sci. 2023;1(1):38–52.